Variations of the scattering ratio in the upper stratosphere over Tomsk in January–March 2000

V.V. Zuev, V.D. Burlakov, A.V. El'nikov, S.V. Smirnov, and P.A. Khryapov

Institute of Atmospheric Optics,
Siberian Branch of the Russian Academy of Sciences, Tomsk

Received September 22, 2000

We present the results of two-wavelength (353 and 511 nm) observations of vertical profiles of the scattering ratio $R(H)$ at the Siberian Lidar Station obtained in January–March 2000. We have recorded an unusual increase in the $R(H)$ ratio in the upper stratosphere at altitudes above 25 km. From analysis of meteorological conditions and the data of double-frequency lidar sensing we discuss the reasons for the observed variations of $R(H)$, whose nature is most likely connected with the development of a sudden stratospheric warming. Such an unusual phenomenon with similar dynamics of the vertical structure of $R(H)$ was observed over Tomsk in the winter of 1987.

Introduction

In the recent few decades laser sensing has been successfully used in the investigations of the spatial and temporal structure of the free atmosphere, its components, and parameters, which reflect the dynamics of its processes. In these investigations particular attention has been given to stratospheric aerosol (SA) as one of the atmospheric components affecting its radiation and thermal regime.[1] Laser sensing of SA can be most simply realized at one wavelength in the optical ranges free from selective absorption by gases. The results of observations show the vertical stratification of SA and, as a rule, are presented as the scattering ratio $R(H)$:

$$R(H) = \frac{\beta_\pi^m(H) + \beta_\pi^a(H)}{\beta_\pi^m(H)}, \qquad (1)$$

where $\beta_\pi^a(H)$ and $\beta_\pi^m(H)$ are the coefficients of aerosol and molecular backscattering, respectively. This parameter demonstrates most clearly the peculiarities in the vertical distribution of stratospheric aerosol.

It has been known that stratospheric aerosol consists of water coated microparticles of sulfuric acid transformed from sulfur dioxide SO_2 or carbonyl sulfide COS entering the stratosphere after volcanic eruptions or under the action of anthropogenic factor. The aerosol sulfate is concentrated in the lower stratosphere, and during several years after huge volcanic eruptions the aerosol sulfate manifests itself as the so-called Junge layer, (the altitude of maximum of this layer correlates with the altitude of the tropopause) located for Tomsk at 18 or 19 km altitude in summer and at 16 or 17 km altitude in winter.[2,3] In the upper stratosphere (above the Junge layer) the aerosol, as a rule, is not observed.

It is for this reason that the 30–35 km altitude range is used to calibrate stratospheric lidars by the molecular scattering signals. Nevertheless, the aerosol formations at altitudes higher than 25 km are sometimes detected, more often in winter. The nature of these formations is associated with the amplification of nucleation and aerosol condensation processes either as a result of variations of the thermodynamic conditions at anomalous temperature rises or when changing the conductivity or ion concentration.[4]

Unusually high values of $R(H)$ at altitudes higher than 25 km were observed at the Siberian Lidar Station in Tomsk (56.5°N, 85.0°E) in January, February, and March 2000. The paper describes the results of laser sensing of the stratosphere during this period as well as the analysis of possible reasons for detecting high values of $R(H)$ in the upper stratosphere.

Methods and lidar facilities for stratospheric lidar observations

In the absence of absorption the lidar equation, relating the lidar return from the path $N(H)$ to the scattering characteristics of atmospheric components, is as follows[5]:

$$N(H) = C\,[\beta_\pi^a(H) + \beta_\pi^m(H)]\,H^{-2} \times \exp\left\{-2\int_0^H [\alpha_m(h) + \alpha_a(h)]\,dh\right\}, \qquad (2)$$

where C is the instrumental constant that includes the parameters of the lidar transmitting and receiving channels; $\alpha_m(h)$ and $\alpha_a(h)$ are the coefficients of the total molecular and aerosol scattering, respectively. When using the calibration method, the determination of $\beta_\pi^a(H)$ and $\alpha_a(h)$ is based on the assumption that

0235-6880/00/11 930-06 $02.00

there is a point H_0 on the sounding path with negligibly low aerosol content (when the aerosol contribution to the total backscatter is less than 2% of the molecular one). Then Eq. (2) takes the form:

$$N(H_0) = C\,\beta_\pi^{\mathrm{m}}(H_0)\,H_0^{-2} \times \exp\left\{-2\int_0^{H_0}[\alpha_{\mathrm{m}}(h) + \alpha_{\mathrm{a}}(h)]\,\mathrm{d}h\right\}. \quad (3)$$

The molecular backscattering coefficient $\beta_\pi^{\mathrm{m}}(H)$ as well as the total molecular scattering coefficient $\alpha_{\mathrm{m}}(h)$ are proportional to the air density $\rho(H)$. The air density can be determined from radiosonde data on temperature. In this case the unknown instrumental constant C is simply determined from Eq. (2). The calibration point H_0 itself is often determined to be in the 25–40 km altitude range from the minimum of the function:

$$F(H) = N(H)\,H^2 \exp\left\{2\int_0^{H}\alpha_{\mathrm{m}}(h)\,\mathrm{d}h\right\} \Big/ \beta_\pi^{\mathrm{m}}(H). \quad (4)$$

The value $\exp\left\{-2\int_{H_0}^{H}\alpha_{\mathrm{a}}(h)\,\mathrm{d}h\right\}$, remained unknown after calibration, introduces an error into the $R(H)$ that is less than 2%.[6]

Unfortunately, the results of aerological sensing of the upper stratosphere are unavailable nowadays in Russia. Therefore we should calibrate the results of laser sensing to model values of $\beta_\pi^{\mathrm{m}}(H)_{\mathrm{mod}}$.[7] Thus, the analyzed profiles of $R(H)$ represent the altitude variation of the net backscattering of the real molecular-aerosol atmosphere relative to the model molecular one. This altitude variation is denoted as $\tilde{R}(H)$.

Lidar observations of the stratosphere over Tomsk were made from January to March 2000 using two setups at the Siberian Lidar Station. Technical parameters of the lidars are shown in Table 1.

Table 1. Lidar parameters

Radiation source	Copper vapor laser	Excimer laser
Wavelength, nm	511	353*
Pulse energy, mJ	1	50
Pulse repetition rate, Hz	2500	60
Time of one profile measurement	25	15
Maximum altitude, km	51.2	102.4
Spatial resolution (time gate), km	0.1	0.1
Field of view of the receiving telescope, mrad	0.6	0.5
Diameter of the primary mirror of the receiving telescope, m	2.2	1

* First Stokes shift of the XeCl-laser radiation at stimulated Raman scattering in the cell with hydrogen at a high pressure.

As is seen from the table, the energy parameters of the lidars differ essentially, therefore the accuracy of the lidar returns recording is different. To improve the statistics of lidar sensing results, the aerosol characteristics were determined from the net lidar signals obtained during the nighttime sensing (on average, 3 or 4 profiles) with the spatial resolution 0.4 km (4 strobes of 0.1 km). To illustrate the high precision characteristics of the lidars used, Figure 1 shows the vertical profiles of the scattering ratio $R(H)$ at two wavelengths of 353 and 511 nm with the confidence interval estimated by the formula $\delta\tilde{R}(H) = \tilde{R}(H)\,\delta N(H)$.

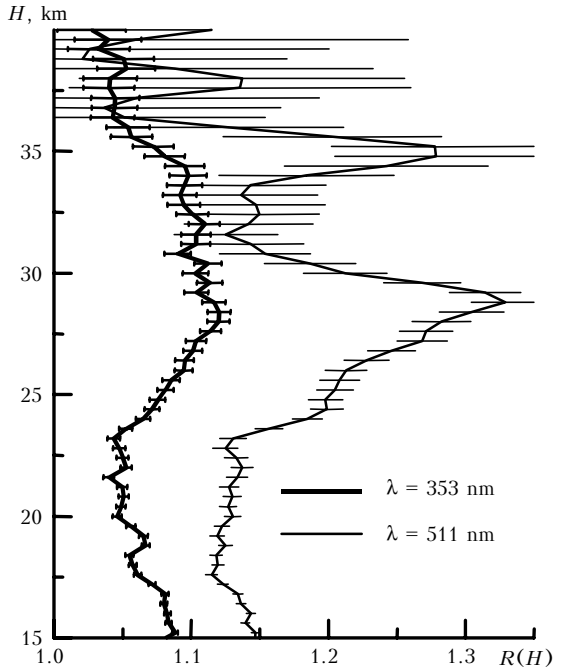

Fig. 1. Profiles of the scattering ratio and their r.m.s. deviations measured on January 26, 2000 (λ = 353 nm) and on January 27, 2000 (λ = 511 nm).

It is evident that the accuracy of $\tilde{R}(H)$ at λ = 353 nm is much higher than that for $\tilde{R}(H)$ at λ = 511 nm. However, the results of lidar sensing at λ = 511 nm with aerosol present a more pronounced vertical stratification of $\tilde{R}(H)$. As a whole, the $\tilde{R}(H)$ profiles at both wavelengths are statistically ensured in all the considered altitude range.

Results of lidar observations

The profiles $\tilde{R}(H)$ obtained from January to March 2000 are shown in Fig. 2. In the figure the $\tilde{R}(H)$ profiles for λ = 353 nm are shown by the bold curve, for λ = 511 nm – by thin curve. It can be seen that on January 21 (Fig. 2*a*) in the whole altitude range the profiles $\tilde{R}(H)$ at both wavelengths are practically the same and are close to unity. This is characteristic of the background aerosol in the stratosphere observed from 1997.[2,8,9] However, the increased values of $\tilde{R}(H) = 1.1$ are observed on

January 26 (Fig. 2*b*) at λ = 353 nm in the altitude range from 23 to 36 km. Practically the same values of $\tilde{R}(H)$ at λ = 353 nm, but showing different vertical stratification still existed on January 27 (Fig. 2*c*). Two distinct local maxima in the aerosol stratification are observed at 24–31 km and 33–37 km altitude, which are more pronounced in the data obtained at λ = 511 nm.

On February 3 (Fig. 2*d*) we observed in the vertical distribution of $\tilde{R}(H)$ an unusual behavior with a minimum at the calibration altitude about 32 km. It can be seen that the value of $\tilde{R}(H)$ increases both in a downward and upward directions from the minimum. In this case, the local maxima of $\tilde{R}(H)$ are well-defined in the altitude range from 20 to 30 km and about 35 km where the peaks of aerosol layers were observed on January 27. A more pronounced bending of the profiles of $\tilde{R}(H)$ with a minimum at 28 km altitude was observed on February 7 (Fig. 2*e*). In this case the profiles of $\tilde{R}(H)$ at both wavelengths of 353 and 511 nm, as a whole, are similar not only in the vertical profile but in the value of $\tilde{R}(H)$.

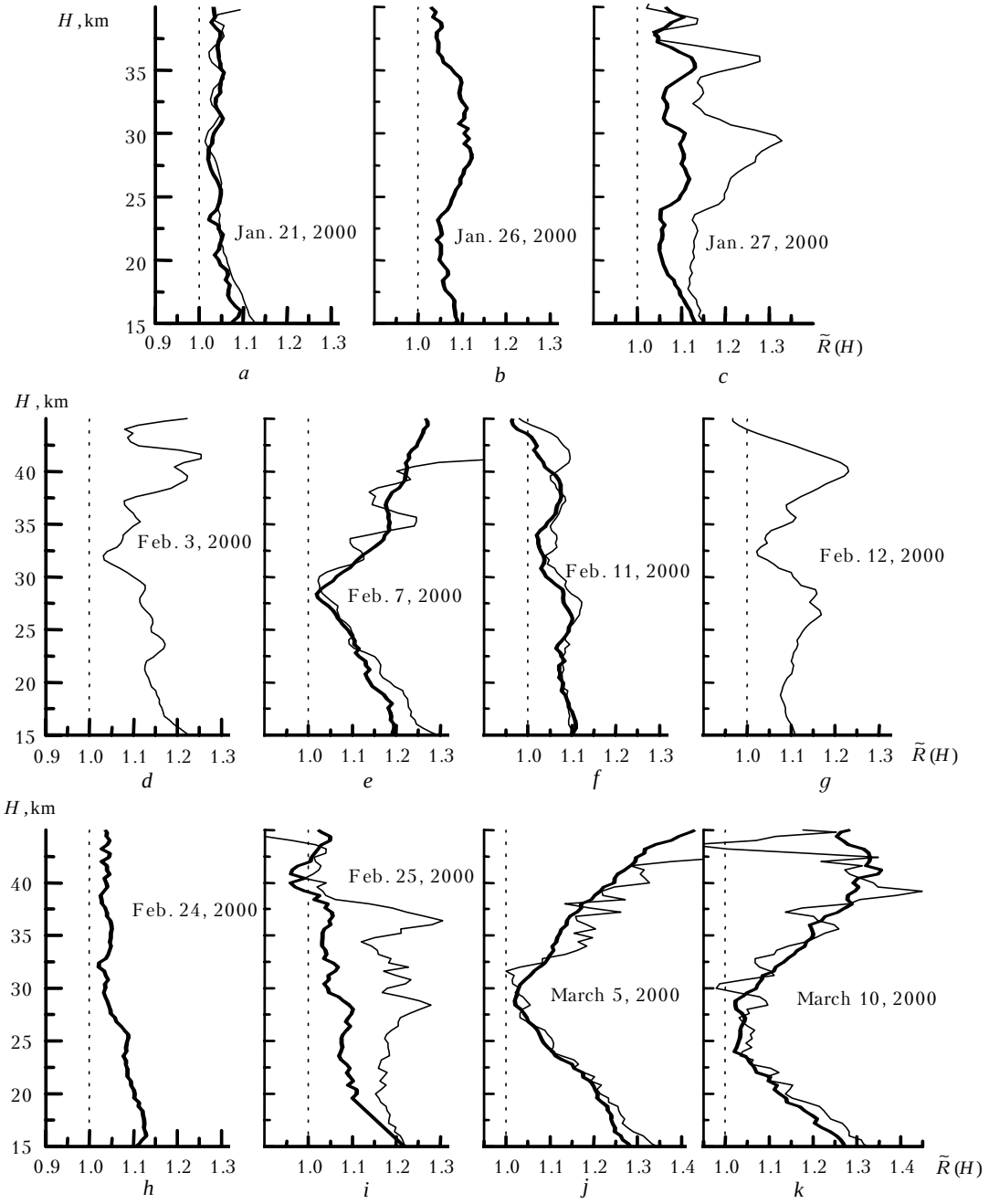

Fig. 2. Profiles of the scattering ratio obtained in January–March 2000 at λ = 353 nm (bold curves) and 511 nm (thin curves).

Subsequent behavior of the profiles $\tilde{R}(H)$, even in fine details, repeats different situations detected in the first half of the period of lidar observations. Thus, the profiles of $\tilde{R}(H)$ on February 11 and 24 (Figs. 2*f* and 2*h*, respectively) repeat the situations of January 21 and 26 (Figs. 2*a* and 2*b*, respectively), and on February 12 and 25 (Figs. 2*g* and 2*i*, respectively)– repeat the situation on January 27 (Fig. 2*c*). Finally, the behavior of $\tilde{R}(H)$ profiles on March 5 and 10 (Fig. 2*j* and 2*k*, respectively) is the same as on February 7 (Fig. 2*e*).

Analysis of results of observations

All the profiles of $\tilde{R}(H)$ obtained may be subdivided into three typical groups. The first group (Figs. 2*c*, 2*g*, and 2*i*), especially at the maxima, is characterized by the condition

$$\tilde{R}(H)_{511} > \tilde{R}(H)_{353} > 1. \quad (5)$$

The second group (Figs. 2*a*, 2*b*, 2*f*, and 2*h*) is characterized by

$$\tilde{R}(H)_{511} \approx \tilde{R}(H)_{353} \approx 1. \quad (6)$$

Finally, the third group (Figs. 2*d*, 2*e*, 2*j*, and 2*k*) for all $H \neq H_0$ satisfies the condition:

$$\tilde{R}(H)_{511} \approx \tilde{R}(H)_{353} > 1. \quad (7)$$

Note that for the molecular scattering the following ratio holds:

$$\frac{\beta_\pi^{\mathrm{m}}(H)_{511}}{\beta_\pi^{\mathrm{m}}(H)_{353}} = \left(\frac{353}{511}\right)^4, \quad (8)$$

and for the aerosol scattering we have, assuming Junge particle size distribution,

$$\frac{\beta_\pi^{\mathrm{a}}(H)_{511}}{\beta_\pi^{\mathrm{a}}(H)_{353}} = \left(\frac{353}{511}\right)^X, \quad (9)$$

where X is the Angström parameter ($X < 4$).

From the analysis of the ratios (1), and (5)–(9) it follows that

a) the condition (5) characterizes real aerosol layers in the stratosphere. The nature of these layers is probably connected with the processes of aerosol formation mentioned in Ref. 4;

b) the condition (6) in the real atmosphere can be fulfilled only in the absence of stratospheric aerosol ($\beta_\pi^{\mathrm{a}}(H)_\lambda \approx 0$) and at the coincidence of model and actual values of $\beta_\pi^{\mathrm{m}}(H)_{\mathrm{mod}} \approx \beta_\pi^{\mathrm{m}}(H)_{\mathrm{real}}$ (or otherwise, the temperature $T(H)$, i.e., $T(H)_{\mathrm{mod}} \approx T(H)_{\mathrm{real}}$);

c) the condition (7), on the one hand, as well as (6), are characterized by the absence of aerosol particles in the stratosphere ($\beta_\pi^{\mathrm{a}}(H)_\lambda \approx 0$). On the other hand, a considerable difference between real temperature and the model ones is available, i.e., $T(H)_{\mathrm{mod}} \neq T(H)_{\mathrm{real}}$. In this case, an unusual altitude behavior of $R(H)$ can be a result of unusual temperature stratification in the stratosphere.

To assess this temperature stratification, one can use the known method of laser sensing of temperature based on the signals due to molecular scattering.[10] It should be noted that the temperature calculation using the above method with the aerosol results in underestimating of the values of the determined temperature. Some temperature profiles, calculated according to lidar returns at $\lambda = 353$ nm with altitude assignment to the model temperature profile[7] at 18 km altitude, are given in Fig. 3. It is seen from the figure that the calculated values of temperatures far exceed the model ones for the upper stratosphere. This temperature excess up to $\Delta T \approx 55$ K can be observed at the warming in the stratosphere. To solve this problem, we use the analysis of meteorological conditions in the stratosphere over Tomsk during the period of lidar observations.

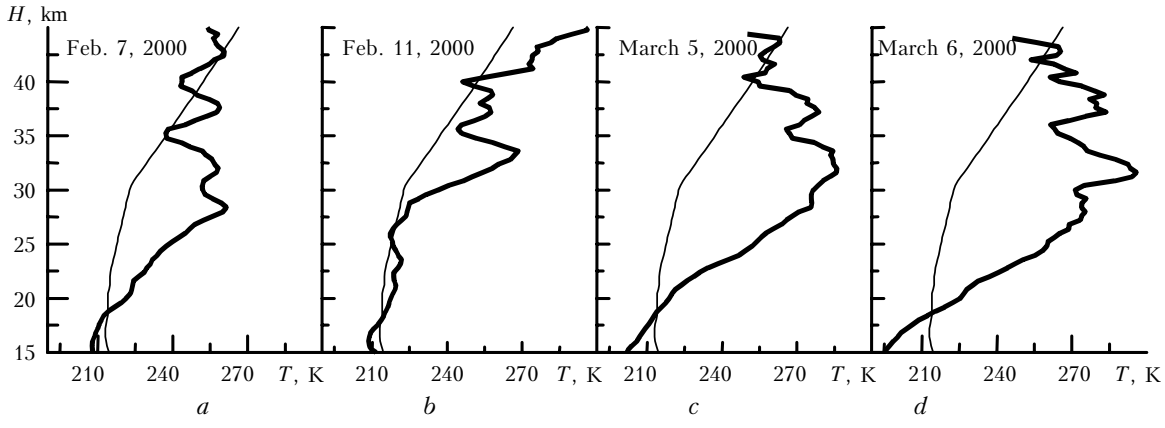

Fig. 3. Vertical profiles of temperature within corresponding days, obtained from lidar data at $\lambda = 353$ nm (bold curve) and the model temperature profile[7] (thin curve).

The available meteorological information over the period from January to March 2000 enables us to distinguish between two periods associated with the blocking processes.[11] The first period is from the end of January to the first decade of February; the second period is from the end of February to the first decade of March. The blocking was caused by the strengthening of the Siberian anticyclone and its motion to high latitudes. This anticyclone is high, warm, and slow and is one of the seasonal centers of atmospheric impact. During this process the macroscale dislocation of zonal transport in the troposphere is accompanied by the increase of wave activity in the stratosphere. When moving to high latitudes, the stratospheric crest of high pressure causes either deformation or shift, or even fragmentation of circumpolar vortex and, accordingly, the disturbance of western zonal transport in the stratosphere. In this case the reconstruction of thermobaric fields is accompanied by cooling of the lower stratosphere while warming the upper stratosphere. A rapid development of such circulation–meteorological conditions can result in the so-called sudden winter stratospheric warming. Under stratospheric warming we observed a sharp increase of temperature by a few tens of degrees during several days.[11,12]

During periods of the maximum development of blocking in the beginning of February and March 2000 Tomsk was inside the warm air tropical mass in the rear part of the baric crest with the cold and high tropopause.

Thus, in the first decade of March the temperature and the position of the tropopause retained about –70°C at the level of 200 hPa. In this case the minimum temperature values reached –75°C, and the tropopause ascended up to the level of 180 hPa. Anomalous-low temperatures were also observed in the lower stratosphere. For example, on March 7 the temperature of –77.3°C was recorded at the aerological sensing station in Aleksandrovskoe (450 km to the north of Tomsk) at the level of 100 hPa. Thus, analysis of meteorological situation has pointed to a well-defined anomalously cold air in the lower stratosphere. At the same time the lidar data (Fig. 3) are indicative of the anomalously warm air in the upper stratosphere. These data with consideration for the well-known regularities of the development of atmospheric processes enable one to confirm the fact of observation, during the winter-spring period 2000, of sudden stratospheric warming over Tomsk.

Conclusion

As was shown by the data of lidar observations and meteorological data analysis, the period of observations from January to March 2000 was most likely in close agreement with the processes of winter stratospheric warming. The rapid dynamics observed in this period of aerosol formations in the upper stratosphere (rapid occurrence and disappearance) of the above formations most likely points to the processes of the first order phase transitions. At the warming weather front the evaporation of water from aerosol particles occurs and in the subsequent cooling the condensation formation of liquid-droplet aerosols takes place.

Sudden stratospheric warming that may cause the extraordinary variations of the scattering ratio is a rare phenomenon at the polar and middle latitudes. In midlatitudes sudden stratospheric warming occurs more rarely.[11,12] Really, the analysis of the entire series of observations of stratospheric aerosol at the Siberian Lidar Station since 1986 up to now has made it possible to determine only one period, for which the dynamics of aerosol and temperature stratification in the stratosphere was similar to the processes occurring from January to March 2000. The profiles of the scattering ratio $R(H)$, calculated from the radiosonde data on temperature, and the profiles of $T(H)$, illustrating the development of the process of stratospheric warming in winter 1987, are given in Fig. 4.

Rapid interrelated height variations of $R(H)$ values and the temperature observed in 1987 and 2000 enable us to assign the aerosol layers in the upper stratosphere to the processes of water vapor re-condensation during the stratospheric cooling after a sudden warming.[4] For example, Fig. 4*a* (01.20.87) shows the anomalous warm up of the stratosphere over Tomsk and the lack of aerosol layers in the upper stratosphere. Figs. 4*b* and *c* show the formation of aerosol layers at altitudes of 27–32 km at the stratospheric cooling after the stratospheric warming. Note that altitude variations of $R(H)$ in 1987 and 2000 under similar conditions differ markedly. Higher values of $R(H)$ obtained in 1987 in the lower stratosphere are associated with the fragments of volcanic aerosol after the eruption of volcanoes of El Chichon (1982) and Del Ruis (1985). Besides, to normalize lidar returns in 1987, the values of $T(H)$ were used measured with radiosondes, and in 2000 the model values of $T(H)$ were used.

The events of recording aerosol layers, originating due to strong variations in the thermodynamic conditions in the stratosphere, being rare in occurrence even for polar and middle latitudes,[11] along with the results of lidar sensing of the ozonosphere during winter periods from 1996 to 1999, presenting the vertical distribution of ozone characteristic of polar latitudes,[13] point to a significant impact of the arctic circumpolar vortex on the stratosphere over Tomsk.

It should also be noted that the analysis of the behavior of the scattering ratio, obtained at two wavelengths, makes it possible to describe a realistic pattern in the stratosphere and to give a correct physical interpretation of lidar data even at significant discrepancies of $T(H)_{\text{mod}} \neq T(H)_{\text{real}}$.

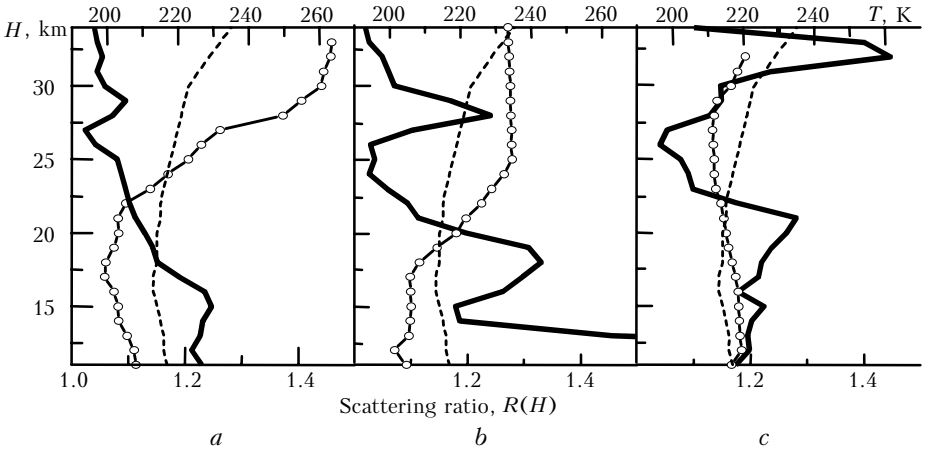

Fig. 4. Profiles of the scattering ratio at λ = 532 (——), the temperature from data of aerological sensing (–o–o–), model temperature profile for mid-latitude winter[7] (– – –) measured on January 20, 1987 (*a*); January 30, 1987 (*b*), and February 22, 1987 (*c*).

Acknowledgments

The authors would like to express their gratitude to A.V. Nevzorov for his assistance in making lidar measurements.

The work has been supported by the Ministry of Science of the Russian Federation and performed at the Siberian Lidar Station (reg. No. 01–64) and partially supported by the Russian Foundation for Basic Research (Grants No. 98–05–64267 and No. 99–05–64943).

References

1. S.S. Khmelevtsov, ed., *Volcanoes, Stratospheric Aerosol and Climate of the Earth* (Gidrometeoizdat, Leningrad, 1986), 256 pp.
2. V.V. Zuev, A.V. El'nikov, and V.D. Burlakov, Atmos. Oceanic Opt. **12**, No. 3, 257–264 (1999).
3. V.V. Zuev, V.D. Burlakov, and A.V. El'nikov, J. Aerosol Sci. **29**, No. 10, 1179–1187 (1998).
4. D.J. Hofmann, J.M. Rosen, and W. Grindell, J. Geophys. Res. **90**, No. D1, 2341–2354 (1985).
5. E.D. Hinkley, ed., *Laser Monitoring of the Atmosphere* (Springer Verlag, New York, 1976).
6. V.N. Marichev and A.V. El'nikov, in: *Proceedings of the IXth All-Union Symposium on Laser and Acoustic Sensing of the Atmosphere* (Publishing House of TA SB AS USSR, Tomsk, 1987), Part I, pp. 154–159.
7. I.I. Ippolitov, V.S. Komarov, and A.A. Mitsel, in: *Spectroscopic Methods of Atmospheric Sensing* (Nauka, Novosibirsk, 1985), pp. 4–44.
8. H. Jager and F. Homburg, in: *Abstracts of Papers at 19th ILRC*, Langley Research Center, Hampton, Virginia (1998), pp. 335–338.
9. G.S. Kent and G.M. Hansen, Appl. Opt. **37**, 3861–3872 (1998).
10. V.V. Zuev, V.N. Marichev, and S.L. Bondarenko, Atmos. Oceanic Opt. **9**, No. 12, 1026–1029 (1996).
11. S.P. Khromov and L.I. Mamontova, *Meteorology Dictionary* (Gidrometeoizdat, Leningrad, 1974), 568 pp.
12. U. von Zank, J. Fiedler, B. Nanjokat, U. Jangematz, and K. Kruger, Geophys. Res. Lett. **25**, No. 22, 4169–4172 (1998).
13. V.V. Zuev, V.N. Marichev, and P.A. Khryapov, Atmos. Oceanic Opt. **12**, No. 7, 607–610 (1999).